SUPPLEMENTARY APPENDIX

Non-muscle myosin II drives vesicle loss during human reticulocyte maturation

Pedro L. Moura,[1] Bethan R. Hawley,[1] Tosti J. Mankelow,[2,3] Rebecca E. Griffiths,[2,3,4] Johannes G.G. Dobbe,[5] Geert J. Streekstra,[5] David J. Anstee,[2,3] Timothy J. Satchwell[1,2,3*] and Ashley M. Toye[1,2,3*]

[1]School of Biochemistry, University of Bristol, UK; [2]Bristol Institute for Transfusion Sciences, National Health Service Blood and Transplant (NHSBT), UK; [3]NIHR Blood and Transplant Research Unit, University of Bristol, UK; [4]UQ-StemCARE, Australian Institute for Bioengineering and Nanotechnology, The University of Queensland, Australia and [5]Department of Biomedical Engineering and Physics, Academic Medical Center, University of Amsterdam, the Netherlands

**These authors contributed equally to this work*

 doi:10.3324/haematol.2018.199083

Received: June 1, 2018.

Accepted: July 26, 2018.

Pre-published: August 3, 2018.

Correspondence: t.satchwell@bristol.ac.uk or ash.m.toye@bristol.ac.uk

SUPPLEMENTAL FIGURES

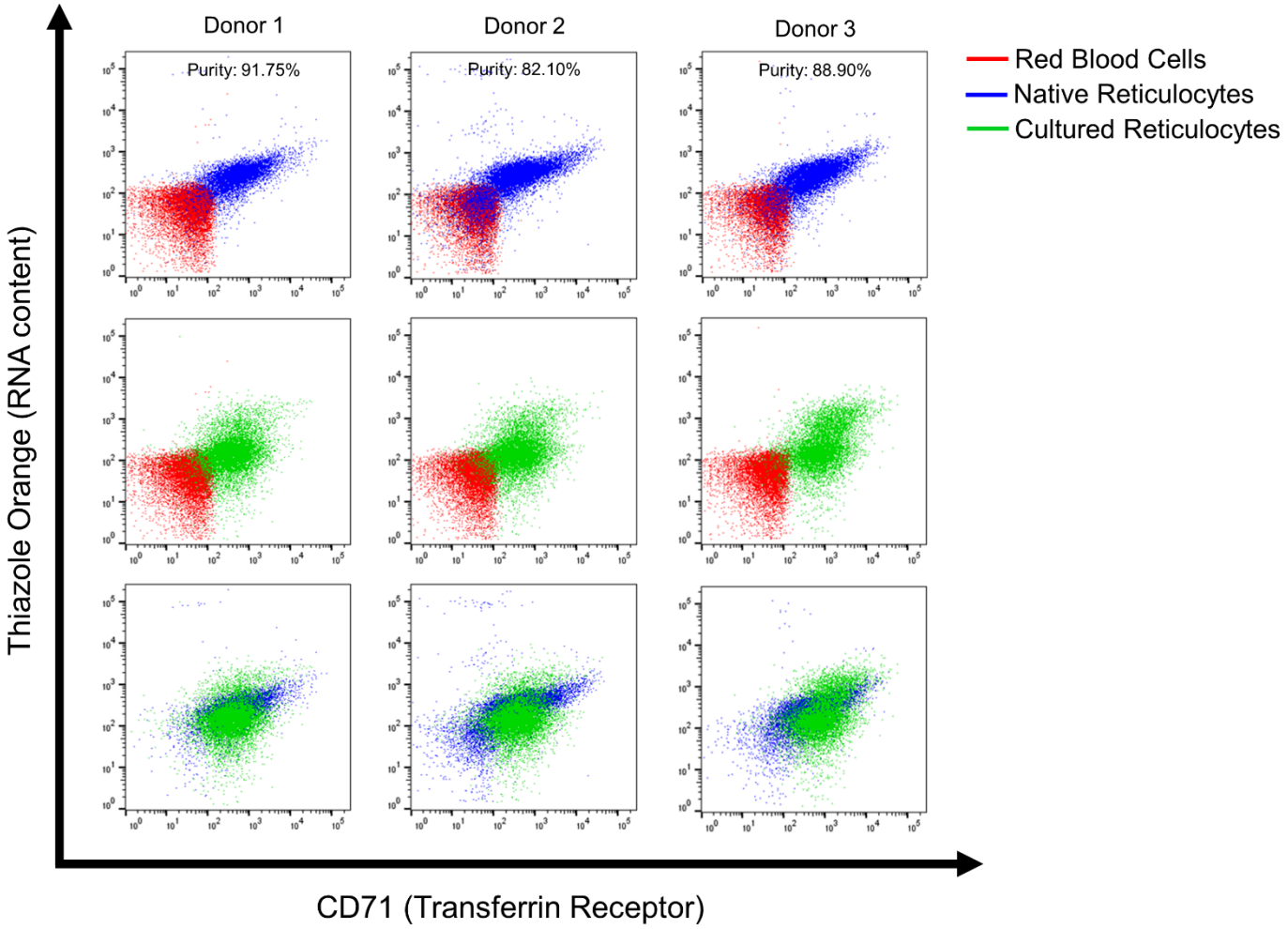

Supplemental Figure 1 – Flow cytometry characterization of samples submitted to proteomics

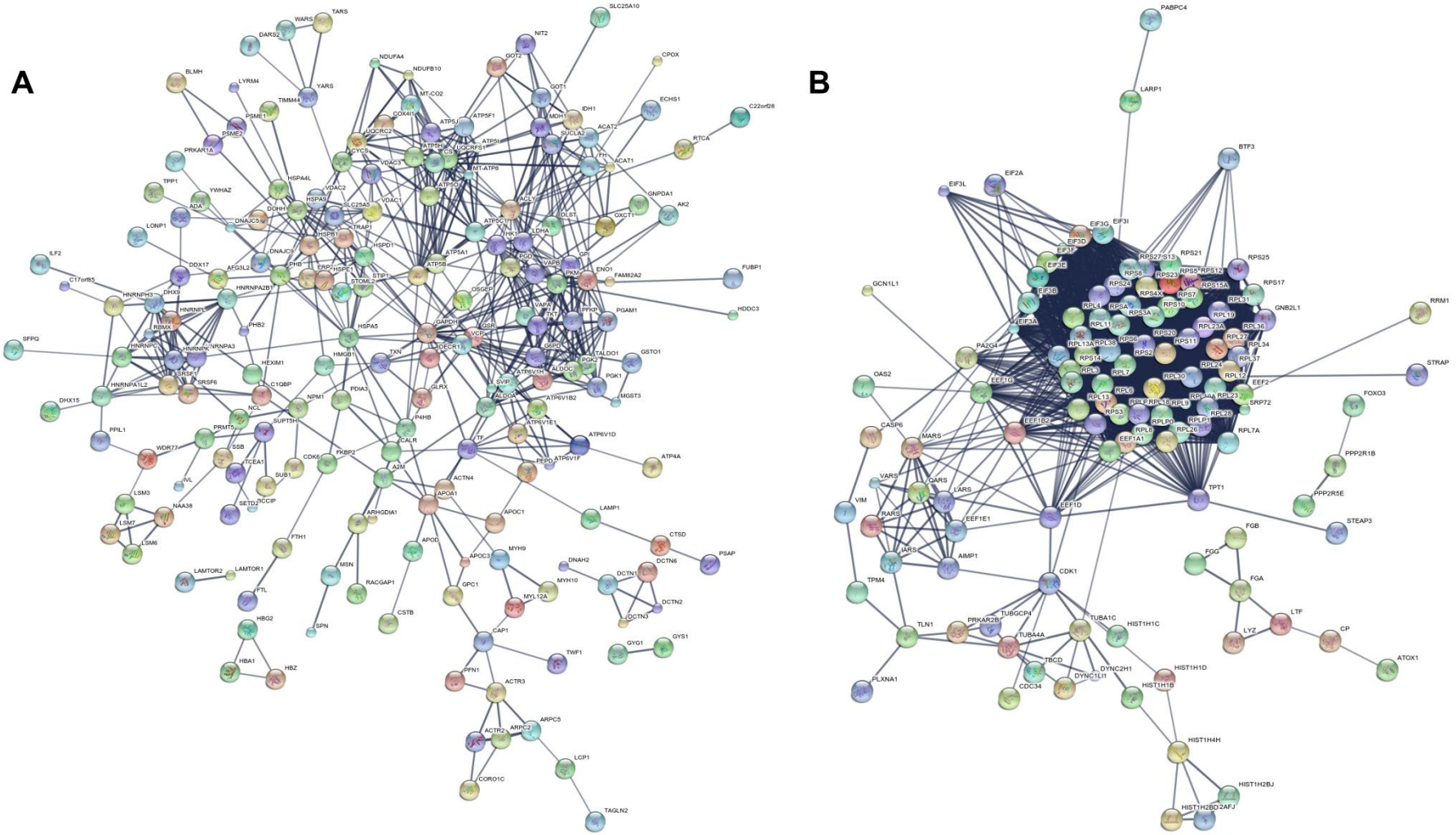

Supplemental Figure 2 – Network analysis of proteomics data

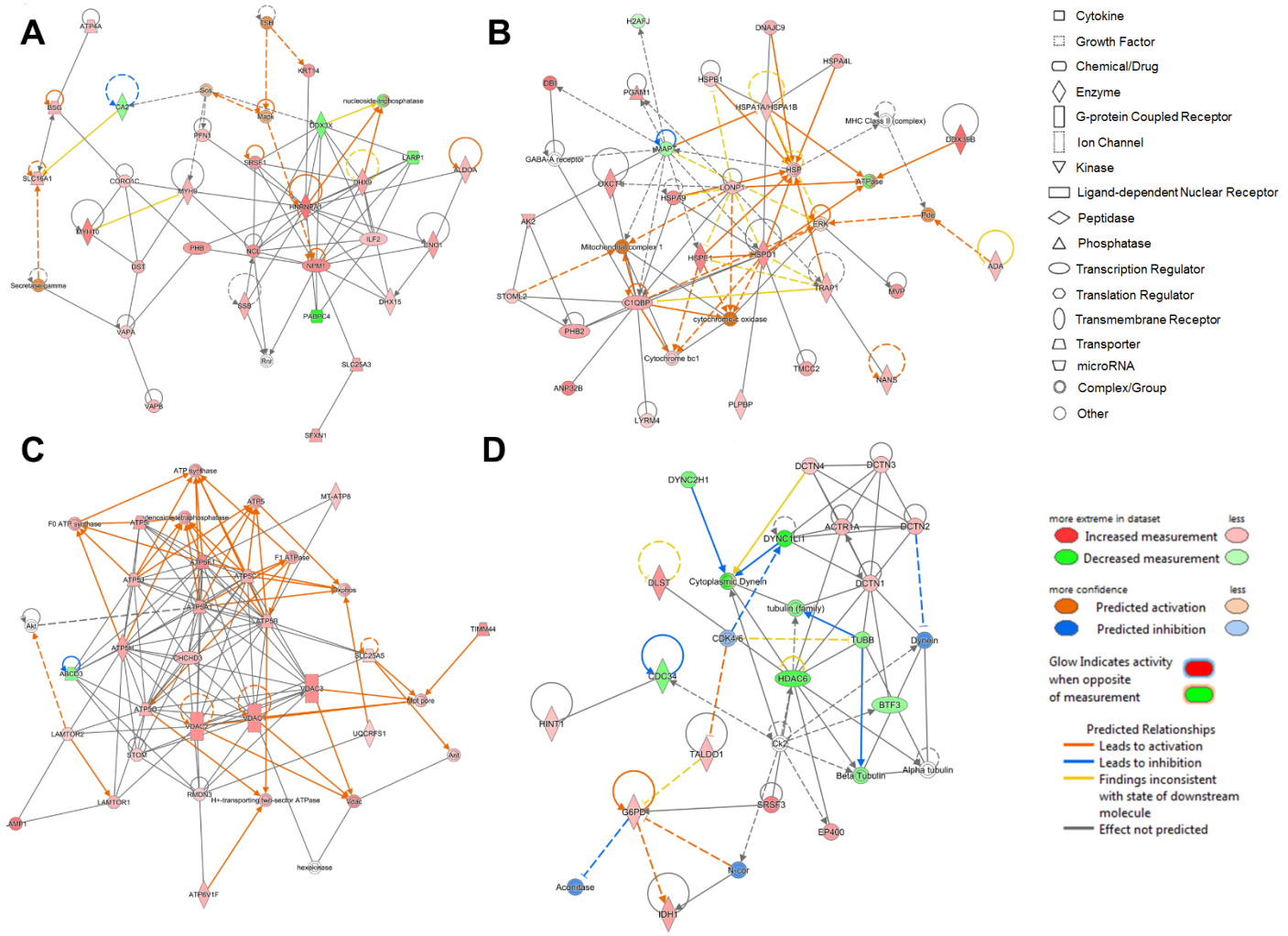

Supplemental Figure 3 – Functional network analysis of proteomics data

A

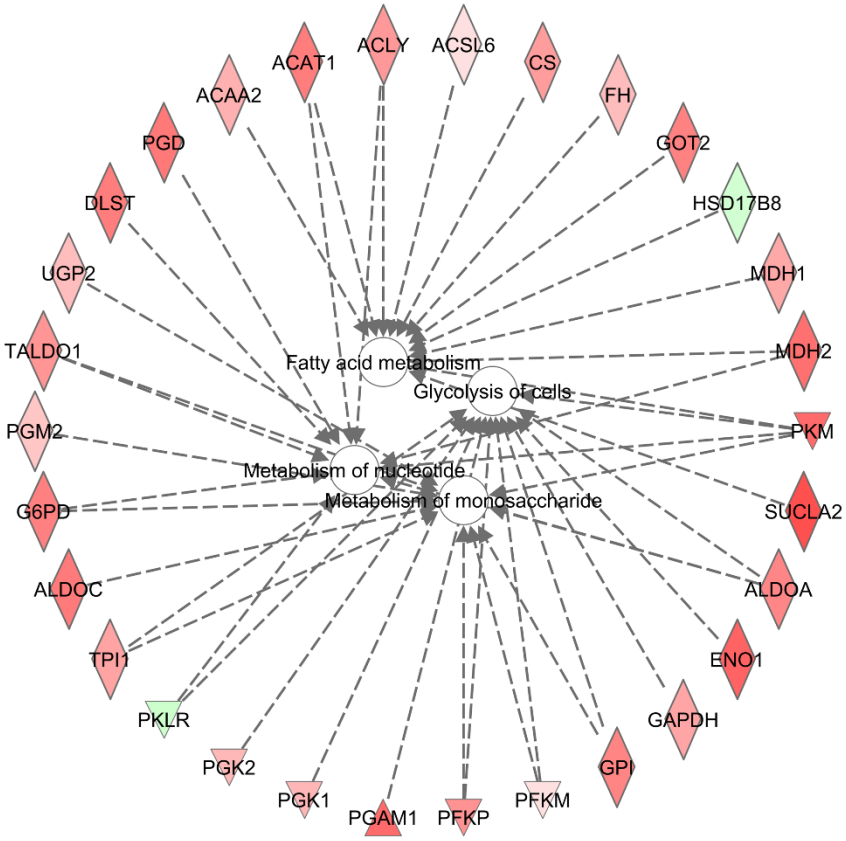

B

Uniprot ID	Symbol	Entrez Gene Name	CultRets_1	CultRets_2	CultRets_3
Q9Y617	PSAT1	Phosphoserine Aminotransferase 1	5.062	2.551	3.707
P04181	OAT	Ornithine Aminotransferase	2.657	2.932	2.496
P29401	TKT	Transketolase	2.11	2.402	1.759
P53602	MVD	Mevalonate Diphosphate Decarboxylase	2.083	2.448	1.46
P06733	ENO1	Enolase 1	1.985	2.34	1.529
P18669	PGAM1	Phosphoglycerate Mutase 1	1.948	2.195	1.445
P36957	DLST	Dihydrolipoamide S-succinyltransferase	2.185	1.928	1.271
P52209	PGD	Phosphogluconate Dehydrogenase	1.965	1.997	1.304
P55809	OXCT1	3-oxoacid Coa-transferase 1	2.151	1.662	1.443
Q0QF37	MDH2	Malate Dehydrogenase 2	1.984	1.715	1.392
Q7Z503	SUCLA2	Succinate-coa Ligase Adp-forming Beta Subunit	0.885	2.413	1.706
B4DE36	GPI	Glucose-6-phosphate Isomerase	1.624	2.023	1.201
P04075	ALDOA	Aldolase, Fructose-bisphosphate A	1.482	2.054	1.179
B3KUZ8	GOT2	Glutamic-oxaloacetic Transaminase 2	1.528	1.842	1.225
P37837	TALDO1	Transaldolase 1	1.479	1.986	1.034
Q59GW6	ACAT2	Acetyl-coa Acetyltransferase 2	1.476	1.839	1.161
A8K8D9	G6PD	Glucose-6-phosphate Dehydrogenase	1.401	1.785	1.244
P24752	ACAT1	Acetyl-coa Acetyltransferase 1	1.725	1.433	1.271
P14618	PKM	Pyruvate Kinase M1/2	1.807	1.033	1.459
P17174	GOT1	Glutamic-oxaloacetic Transaminase 1	1.484	1.783	0.847
P09972	ALDOC	Aldolase, Fructose-bisphosphate C	1.516	1.302	1.295
Q01813	PFKP	Phosphofructokinase, Platelet	1.264	1.773	1.058
Q2TSD0	GAPDH	Glyceraldehyde-3-phosphate Dehydrogenase	1.541	1.666	0.878
A0A0B4J2A4	ACAA2	Acetyl-coa Acyltransferase 2	1.535	1.667	0.764
P53396	ACLY	ATP Citrate Lyase	1.126	1.84	1
P40925	MDH1	Malate Dehydrogenase 1	1.211	1.866	0.844
V9HWK1	TPI1	Triosephosphate Isomerase 1	1.24	1.663	0.895
P30084	ECHS1	Enoyl-coa Hydratase, Short Chain 1	1.261	1.483	0.81
Q8N5Y3	GYG1	Glycogenin 1	1.181	1.604	0.727
A0A087WYS1	UGP2	Udp-glucose Pyrophosphorylase 2	1.157	1.61	0.647
P00558	PGK1	Phosphoglycerate Kinase 1	1.103	1.533	0.713
P07205	PGK2	Phosphoglycerate Kinase 2	1.209	1.403	0.687
A8K6K7	GYS1	Glycogen Synthase 1	0.706	1.328	1.247
P07954	FH	Fumarate Hydratase	1.095	1.5	0.656
B4DJV2	CS	Citrate Synthase	1.089	1.151	0.955
Q99714	HSD17B10	Hydroxysteroid 17-beta Dehydrogenase 10	0.492	1.183	1.164
Q96G03	PGM2	Phosphoglucomutase 2	0.876	1.273	0.553
Q04446	GBE1	1,4-alpha-glucan Branching Enzyme 1	0.56	1.159	0.516
Q05DJ2	MTAP	Methylthioadenosine Phosphorylase	0.691	1.111	0.344
P08237	PFKM	Phosphofructokinase, Muscle	0.592	1.304	0.248
G1UI17	AGL	Amylo-alpha-1, 6-glucosidase	0.247	0.935	0.903
P11216	PYGB	Glycogen Phosphorylase B	0.747	0.811	0.303
B2RB06	HADH	Hydroxyacyl-coa Dehydrogenase	0.176	0.657	0.719
B4DWX6	ACADM	Acyl-coa Dehydrogenase Medium Chain	0.13	0.638	0.66
P40939	HADHA	Hydroxyacyl-coa Dehydrogenase	0.463	0.375	0.575
E7ERD7	ACSL6	Acyl-coa Synthetase Long Chain Family 6	0.139	0.81	0.088
Q6PCE3	PGM2L1	Phosphoglucomutase 2 Like 1	0.255	0.664	0.11
B4DY96	HADHB	Hydroxyacyl-coa Dehydrogenase Subunit Beta	0.042	0.204	0.309
P21399	ACO1	Aconitase 1	-0.048	0.541	-0.107
P30613	PKLR	Pyruvate Kinase L/R	-0.295	0.278	-0.438
B4DZ08	ACO2	Aconitase 2	-0.919	0.069	-0.453
Q92506	HSD17B8	Hydroxysteroid 17-beta Dehydrogenase 8	-1.115	-0.449	-0.402
A0A024R7A5	MGAM	Maltase-glucoamylase	-1.643	-2.353	-1.991

Supplemental Figure 4 – Cultured reticulocytes are more metabolically active than native reticulocytes

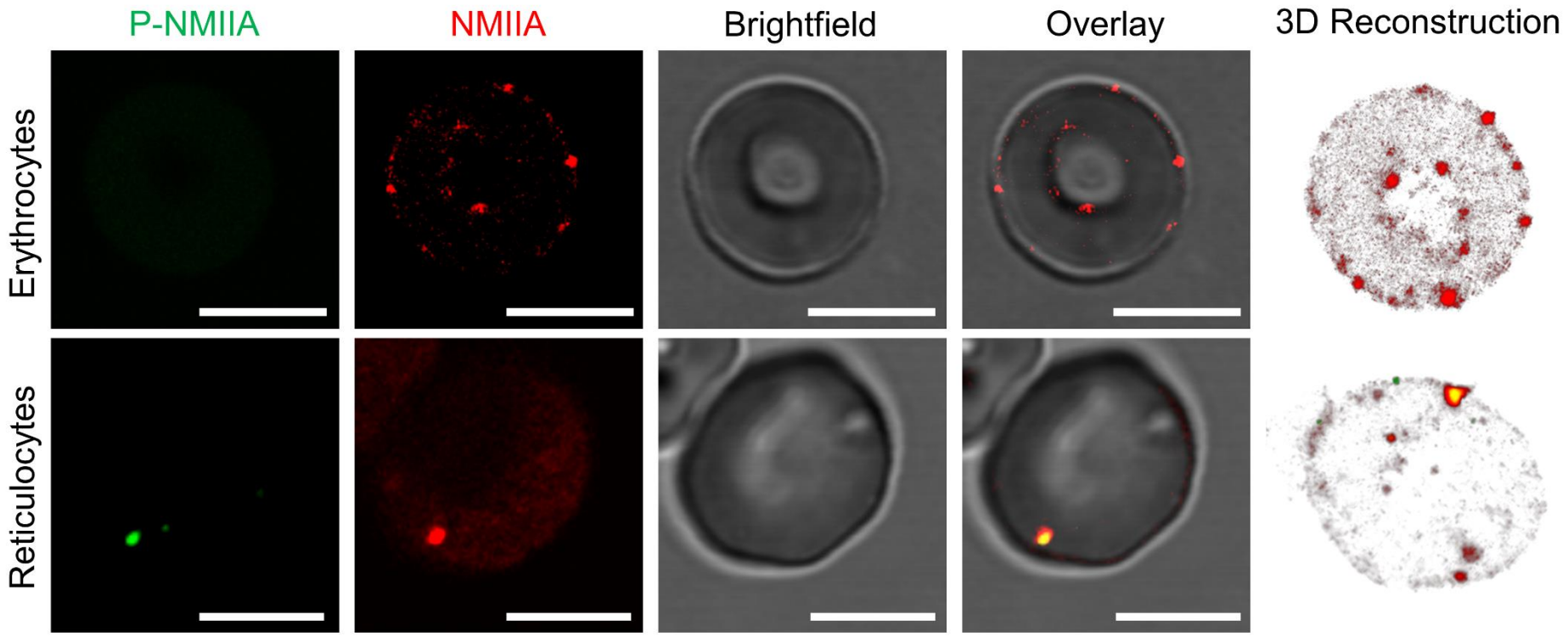

Supplemental Figure 5 – NMIIA has differential localization in the erythrocyte and reticulocyte

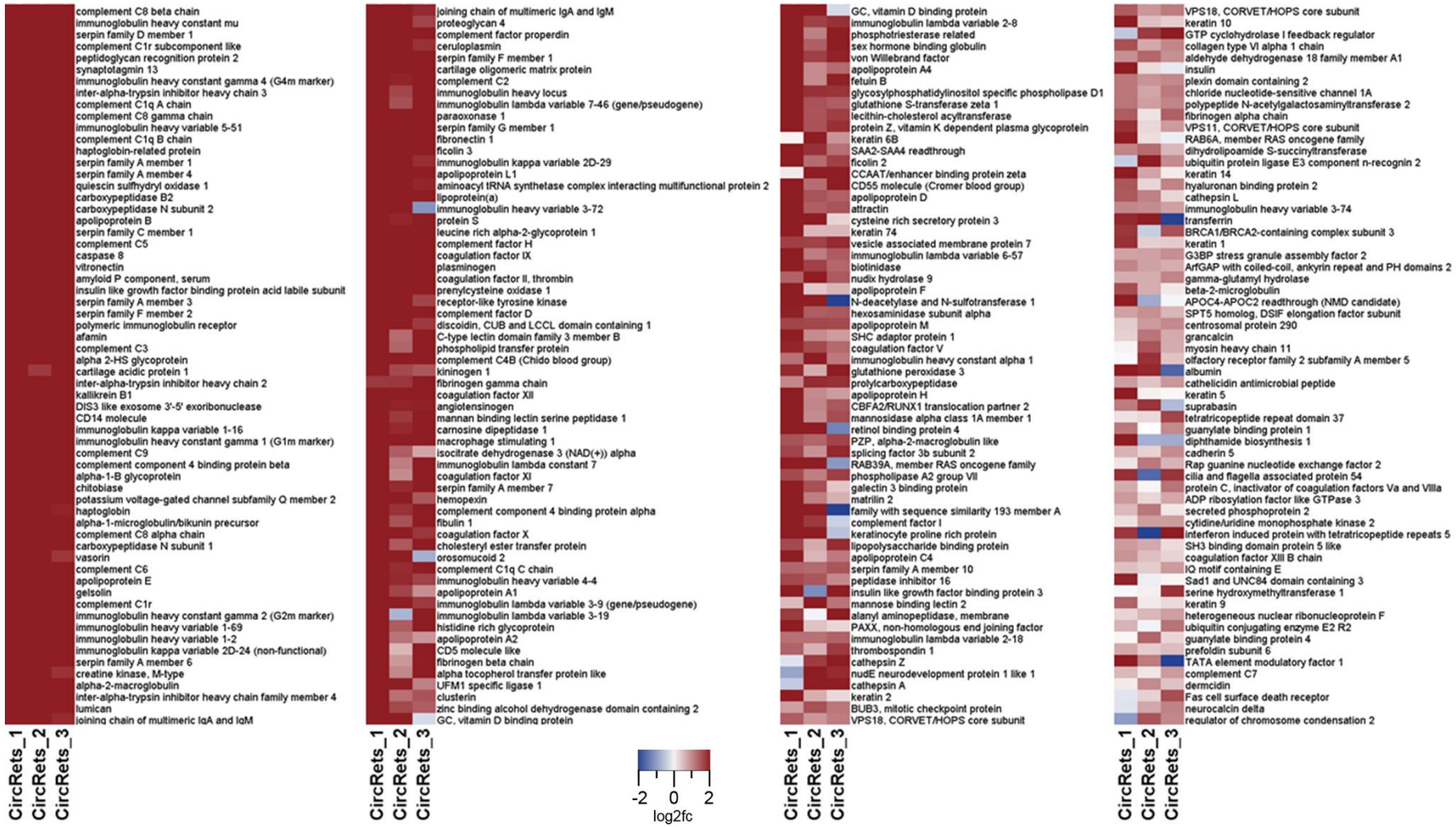

Supplemental Figure 6 – Preferentially retained proteins in circulated reticulocytes

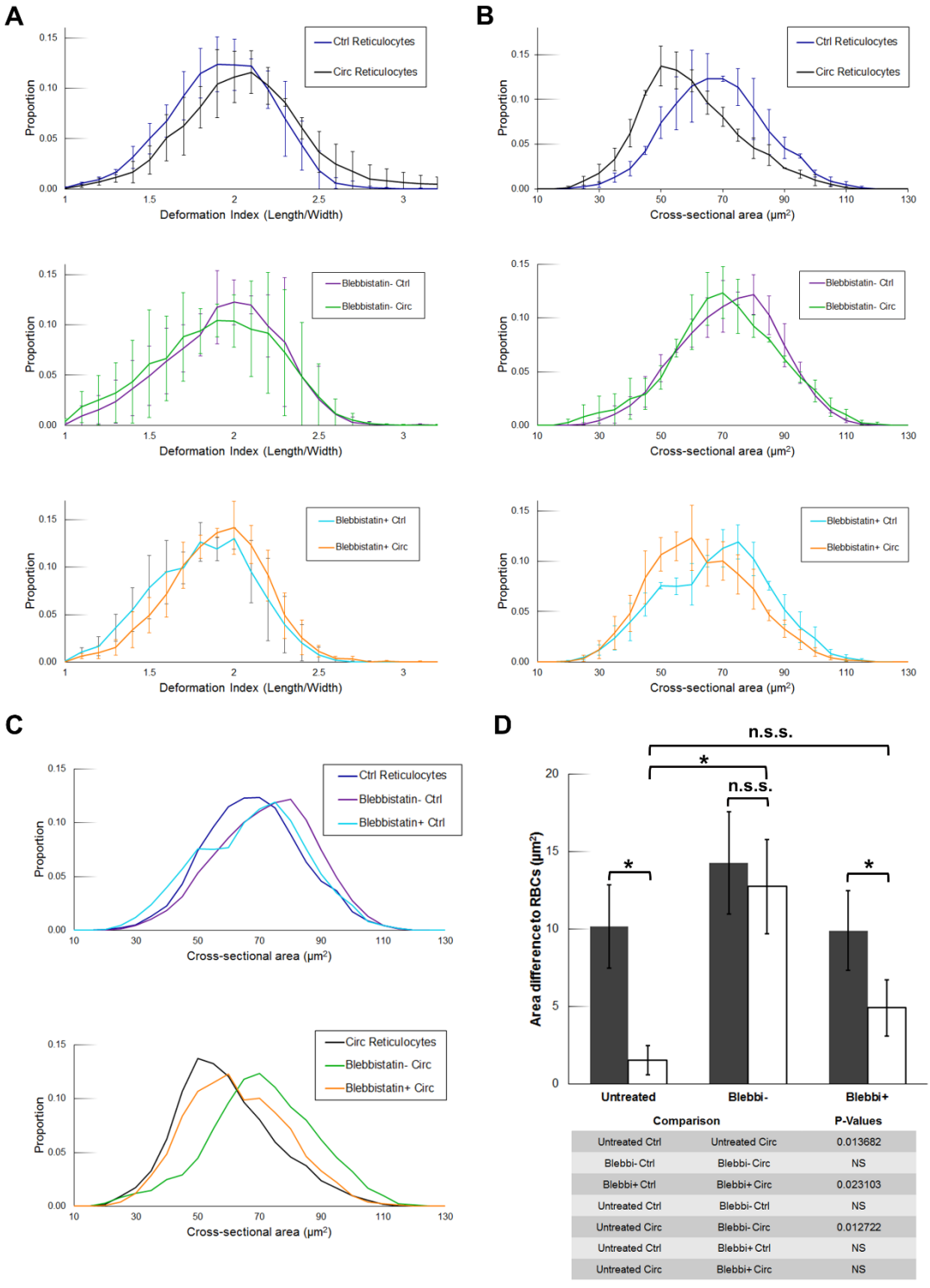

Comparison		P-Values
Untreated Ctrl	Untreated Circ	0.013682
Blebbi- Ctrl	Blebbi- Circ	NS
Blebbi+ Ctrl	Blebbi+ Circ	0.023103
Untreated Ctrl	Blebbi- Ctrl	NS
Untreated Circ	Blebbi- Circ	0.012722
Untreated Ctrl	Blebbi+ Ctrl	NS
Untreated Circ	Blebbi+ Circ	NS

Supplemental Figure 7 - Blebbistatin treatment abrogates circulation-induced differences in reticulocyte cross-sectional area

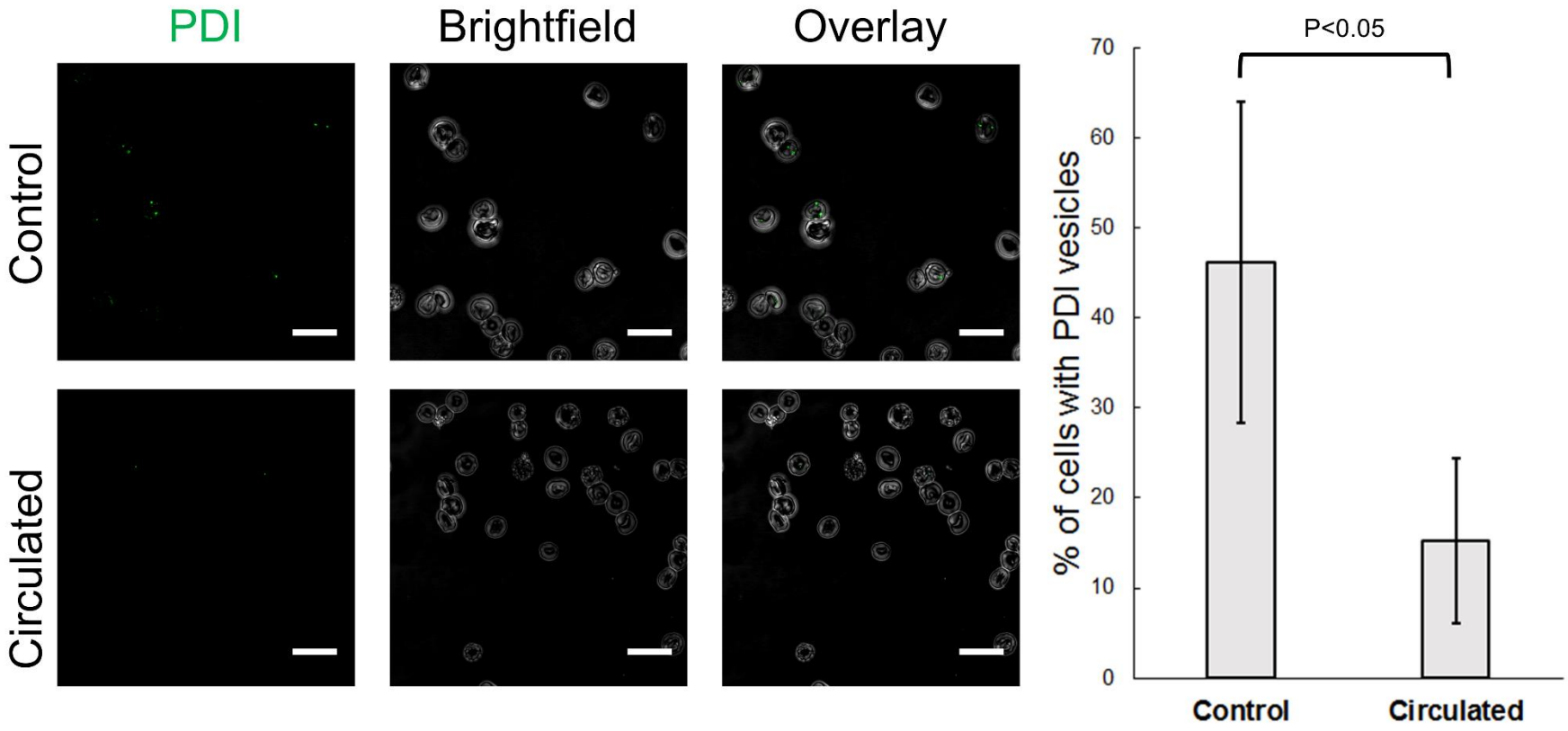

Supplemental Figure 8 – Circulation of cultured reticulocytes leads to vesicle loss

SUPPLEMENTAL FIGURE LEGENDS

Supplemental Figure 1 – Flow cytometry characterization of samples submitted to proteomics

Flow cytometry analysis of native reticulocytes, cultured reticulocytes and red blood cells stained with thiazole orange and anti-CD71 antibody. Purity of the CD71 isolation protocol for each individual donor is written under their identification, defined as the $TO^-/CD71^-$ percentage of the cell population. Pairwise comparisons are shown for ease of visualization.

Supplemental Figure 2 – Network analysis of proteomics data

Protein network of A) upregulated and B) downregulated proteins in cultured reticulocytes in relation to endogenous reticulocytes. Networks were generated via use of the STRING database, medium confidence settings.

Supplemental Figure 3 – Functional network analysis of proteomics data

Top scoring protein networks in a comparison of cultured reticulocytes in relation to endogenous reticulocytes. The dataset was filtered to remove protein families with a large number of proteins (ribosomal proteins, initiation factors and tRNA synthetases), and networks were generated with the use of the Ingenuity Pathway Analysis software. Networks A, B, C and D correspond to networks 1 through 4 in **Sup. Table 1**, respectively. Red denotes higher abundance in cultured reticulocytes and green denotes higher abundance in endogenous reticulocytes. Orange and blue correspond to predicted up or downregulated interactions in the protein-protein interaction network, respectively. Since IPA is optimized for gene expression analysis, some inconsistencies in the prediction algorithm occur with our non-transcriptionally active erythrocyte dataset, which are symbolized in yellow. Shape legends are displayed within the figure.

Supplemental Figure 4 – Cultured reticulocytes are more metabolically active than native reticulocytes

A) Visualization of proteins generated from $\log_2$ fold change values of the reticulocyte comparison dataset, clustered by metabolic function. Red denotes higher abundance in cultured reticulocytes and green denotes higher abundance in endogenous reticulocytes. Shape legends are displayed in **Supplemental Figure 3**. B) Table displaying proteins present in enriched metabolic pathways through IPA analysis, listed by descending average $\log_2$ fold change. UniProt ID, gene symbol, protein name and $\log_2$ fold change for each sample of cultured reticulocytes versus native reticulocytes are displayed.

Supplemental Figure 5 – NMIIA has differential localization in the erythrocyte and reticulocyte

Erythrocytes (top) and cultured reticulocytes (bottom) were co-labelled for Phospho-Non-Muscle Myosin IIA (S1943) (green) and Non-Muscle Myosin IIA (NMIIA) (red) and subjected to confocal imaging. Cells were fixed, labelled and cytospun as described in the Materials and Methods. Scale bars: 5 μm.

Supplemental Figure 6 – Preferentially retained proteins in circulated reticulocytes

Heatmap visualization of the preferentially retained subset of the TMT proteome dataset generated from $\log_2$ fold change values of expression in circulated reticulocytes with uncirculated reticulocytes as a baseline. Individual samples were visualized as separate rows. Blue denotes lower expression, and red denotes higher expression. Proteins are displayed vertically by order of average $\log_2$ fold change.

Supplemental Figure 7 - Blebbistatin treatment abrogates circulation-induced differences in reticulocyte cross-sectional area

A) Deformability index (Length/Width ratio) profile of uncirculated and circulated cultured reticulocytes left untreated or treated with Blebbistatin(-) or Blebbistatin(+). The profile is plotted as the average of the proportion of cells within each deformability index “bin” (corresponding to 0.1 ratio units). Error bars correspond to the standard deviation of each average. Data was obtained using the ARCA.

B) Cross-sectional area profile of uncirculated and circulated reticulocytes left untreated or treated with Blebbistatin(-) or Blebbistatin(+). The profile is plotted as the average of the proportion of cells within each area “bin” (corresponding to 5μm^2). Error bars correspond to the standard deviation of each average. Data was obtained using the ARCA.

C) Overlay of the cross-sectional area average profiles of all samples corresponding to uncirculated (top) and circulated (bottom) reticulocytes. Error bars were removed for ease of visualization.

D) Comparison of the area difference to RBCs between untreated, Blebbistatin(-) and Blebbistatin(+) treated cells that were left in culture (grey) or were circulated overnight (white). * indicates a P-value of under 0.05, with n.s.s. (not statistically significant) indicating P-values above 0.05. P-values for relevant comparisons are shown underneath the graph. All comparisons were made with paired two-tailed T-test between arrays of area difference to RBCs. Data are represented as mean ± SD (n=3).

Supplemental Figure 8 – Circulation of cultured reticulocytes leads to vesicle loss

Comparison of the proportion of reticulocytes with vesicles containing Protein Disulphide isomerase before and after circulation using manual counting with the Vision4D software. The displayed immunofluorescence images are representative Z-projections of the observed signal (scale bar = 20 µm). A minimum of 100 cells were counted per each repeat. Data are represented as mean ± SD (n=3).

SUPPLEMENTAL TABLE LEGENDS

Supplemental Table 1 – Quantified differences in protein abundance between erythrocytes, native reticulocytes and cultured reticulocytes

Columns include: UniProt accession number, Protein identification, score, coverage, number of unique peptides and global peptides identified per protein, number of peptide spectrum matches, number of aminoacids, molecular weight, calculated isoelectric point and relative abundance between sample pairs. FDR = 5%.

Supplemental Table 2 - Functional network analysis of proteomics data

Functional protein networks found in a comparison of cultured reticulocytes in relation to endogenous reticulocytes after analysis with the Ingenuity Pathway Analysis software.

Supplemental Table 3 – Phosphoproteins and phosphopeptides identified in erythrocytes, native reticulocytes and cultured reticulocytes

Columns in the protein table include: UniProt accession number, Protein identification, score, coverage, number of unique peptides and global peptides identified per protein, number of peptide spectrum matches, number of aminoacids, molecular weight, calculated isoelectric point and relative abundance between sample pairs. Columns in the peptide table include peptide sequence, PSM ambiguity, number of proteins and protein groups, modifications identified and MS peptide-specific data. FDR = 5%.

Supplemental Table 4 - Quantified differences in protein abundance between cultured uncirculated and *ex vivo* circulated reticulocytes

Columns include: UniProt accession number, Protein identification, score, coverage, number of unique peptides and global peptides identified per protein, number of peptide spectrum matches, number of aminoacids, molecular weight, calculated isoelectric point and relative abundance between sample pairs. FDR = 5%.

SUPPLEMENTAL METHODS

Antibodies

Rabbit polyclonal anti-phospho-Myosin Heavy Chain 2A (MYH9/NMIIA) (Ser1943 - AB2974; Millipore, Burlington, USA) and mouse monoclonal anti-MYH9/NMIIA (GTX633295; GeneTex, Irvine, USA) were used at 1:1000 dilution for western blot and 1:200 dilution for confocal microscopy. Monoclonal mouse antibody BRIC273 (anti-protein 4.2; IBGRL Research Products, Bristol, UK) was used at 1:1000 dilution for western blot as a loading control. Monoclonal mouse anti-LC3B (ALX-803-080-C100; Enzo, Farmingdale, SA), monoclonal mouse anti-PDI (clone 1D3, ADI-SPA-891; Enzo), monoclonal mouse anti-GPA (clone R10, IBGRL Research Products), polyclonal rabbit anti-Calreticulin (ab2907; Abcam, Cambridge, UK), polyclonal rabbit anti-LAMP1 (ab24170; Abcam), polyclonal rabbit anti-Giantin (PRB-114C; BioLegend, San Diego, USA) and polyclonal rabbit anti-phospho-Myosin Light Chain (Ser20 – ab2480, Abcam) were used at 1:200 dilution for confocal microscopy (ALX-803-080-C100; Enzo).

Secondary antibodies used were Alexa-488™, Alexa594™ or Alexa647™ conjugated goat anti-mouse or anti-rabbit (Life Technologies, Carlsbad, USA) at a 1:400 dilution for immunofluorescence and HRP-conjugated rabbit anti-mouse and swine anti-rabbit (Dako, Ely, UK) at 1:1000 dilution for immunoblotting. For the co-labelling of PDI and R10, a Fab fragment rabbit anti-mouse antibody (315-007-003; Jackson ImmunoResearch, West Grove, USA) was employed at 1:10 dilution between labelling protocols to enable co-labelling with two monoclonal mouse antibodies.

TMT Labelling and High pH Reversed-phase Chromatography

Aliquots of 100µg protein of six or nine samples per experiment were digested with trypsin (2.5µg trypsin per 100µg protein; 37°C, overnight), labelled with Tandem Mass Tag (TMT) six or ten plex reagents according to the manufacturer's protocol (Thermo Fisher Scientific) and the labelled samples pooled.

An aliquot of the pooled sample was evaporated to dryness, resuspended in 5% formic acid and then desalted using SepPak cartridges according to the manufacturer's instructions (Waters, Milford, USA). Eluate from the SepPak cartridge was again evaporated to dryness and resuspended in buffer A (20 mM ammonium hydroxide, pH 10) prior to fractionation by high pH reversed-phase chromatography using an Ultimate 3000 liquid chromatography

system (Thermo Fisher Scientific). In brief, the sample was loaded onto an XBridge BEH C18 Column (130Å, 3.5 µm, 2.1 mm X 150 mm, Waters, UK) in buffer A and peptides eluted with an increasing gradient of buffer B (20 mM Ammonium Hydroxide in acetonitrile, pH 10) from 0-95% over 60 min. The resulting fractions were evaporated to dryness and resuspended in 1% formic acid prior to analysis by nano-LC MSMS using an Orbitrap Fusion Tribrid mass spectrometer (Thermo Fisher Scientific).

Nano-LC Mass Spectrometry

High pH RP fractions were further fractionated using an Ultimate 3000 nano-LC system in line with an Orbitrap Fusion Tribrid mass spectrometer (Thermo Fisher Scientific). In brief, peptides in 1% (v/v) formic acid were injected onto an Acclaim PepMap C18 nano-trap column (Thermo Fisher Scientific). After washing with 0.5% (v/v) acetonitrile 0.1% (v/v) formic acid peptides were resolved on a 250 mm × 75 µm Acclaim PepMap C18 reverse phase analytical column (Thermo Fisher Scientific) over a 150 min organic gradient, using 7 gradient segments (1-6% solvent B over 1 min., 6-15% B over 58 min., 15-32%B over 58 min., 32-40%B over 5 min., 40-90%B over 1 min., held at 90%B for 6 min and then reduced to 1%B over 1 min.) with a flow rate of 300 nl min−1. Solvent A was 0.1% formic acid and Solvent B was aqueous 80% acetonitrile in 0.1% formic acid. Peptides were ionized by nano-electrospray ionization at 2.0kV using a stainless-steel emitter with an internal diameter of 30 µm (Thermo Fisher Scientific) and a capillary temperature of 275°C. All spectra were acquired using an Orbitrap Fusion Tribrid mass spectrometer controlled by Xcalibur 2.0 software (Thermo Fisher Scientific) and operated in data-dependent acquisition mode using an SPS-MS3 workflow. FTMS1 spectra were collected at a resolution of 120,000, with an automatic gain control (AGC) target of 400,000 and a max injection time of 100ms. Precursors were filtered with an intensity range from 5,000 to 1E20, according to charge state (to include charge states 2-6) and with monoisotopic precursor selection. Previously interrogated precursors were excluded using a dynamic window (60s +/-10ppm). The MS2 precursors were isolated with a quadrupole mass filter set to a width of 1.2m/z. ITMS2 spectra were collected with an AGC target of 10 000, max injection time of 70ms and CID collision energy of 35%.

For FTMS3 analysis, the Orbitrap was operated at 30,000 resolution with an AGC target of 50,000 and a max injection time of 105ms. Precursors were fragmented by high energy collision dissociation (HCD) at a normalised collision energy of 55% to ensure maximal TMT reporter ion yield. Synchronous Precursor Selection (SPS) was enabled to include up to 5 MS2 fragment ions in the FTMS3 scan.

Phosphoproteomics Sample Processing

The samples were separated using SDS-PAGE, allowing the dye front to run approximately 1cm into the separating gel and the gel piece was then subjected to in-gel tryptic digestion using a DigestPro automated digestion unit (Intavis Ltd). The resulting peptides were then subjected to TiO2-based phosphopeptide enrichment according to the manufacturer's instructions (Pierce).

Enriched phosphopeptides were fractionated using an Ultimate 3000 nano-LC system in line with an Orbitrap Fusion Tribrid mass spectrometer (Thermo Fisher Scientific). In brief, peptides in 1% (v/v) formic acid were injected onto an Acclaim PepMap C18 nano-trap column (Thermo Fisher Scientific). After washing with 0.5% (v/v) acetonitrile 0.1% (v/v) formic acid peptides were resolved on a 250 mm × 75 μm Acclaim PepMap C18 reverse phase analytical column (Thermo Fisher Scientific) over a 150 min organic gradient, using 7 gradient segments (1-6% solvent B over 1 min., 6-15% B over 58 min., 15-32%B over 58 min., 32-40%B over 5 min., 40-90%B over 1 min., held at 90%B for 6 min and then reduced to 1%B over 1 min.) with a flow rate of 300 nl min−1. Solvent A was 0.1% formic acid and Solvent B was aqueous 80% acetonitrile in 0.1% formic acid. Peptides were ionized by nano-electrospray ionization at 2.2 kV using a stainless-steel emitter with an internal diameter of 30 μm (Thermo Scientific) and a capillary temperature of 250°C.

All spectra were acquired using an Orbitrap Fusion Tribrid mass spectrometer controlled by Xcalibur 2.0 software (Thermo Fisher Scientific) and operated in data-dependent acquisition mode. FTMS1 spectra were collected at a resolution of 120,000 over a scan range (m/z) of 350-1,550, with an automatic gain control (AGC) target of 400,000 and a max injection time of 100ms. The Data Dependent mode was set to Cycle Time with 3s between master scans. Precursors were filtered according to charge state (to include charge states 2-7) and with monoisotopic precursor selection. Previously interrogated precursors were excluded using a dynamic window (40s +/-10ppm). The MS2 precursors were isolated with a quadrupole mass filter set to a width of 1.6m/z. ITMS2 spectra were collected with an AGC target of 5,000, max injection time of 50ms and HCD collision energy of 35%.

Proteomics Raw Data Processing

TMT Analysis: The raw data files were processed and quantified using Proteome Discoverer software v2.1 (Thermo Fisher Scientific) and searched against the UniProt Human database (134,169 entries) using the SEQUEST algorithm. Peptide precursor mass tolerance was set at 10ppm, and MS/MS tolerance was set at 0.6Da. Search criteria included oxidation of methionine (+15.9949) as a variable modification and carbamidomethylation of cysteine

(+57.0214) and the addition of the TMT mass tag (+229.163) to peptide N-termini and lysine as fixed modifications. Searches were performed with full tryptic digestion and a maximum of 1 missed cleavage was allowed. The reverse database search option was enabled and all peptide data was filtered to satisfy false discovery rate (FDR) of 5%.

Phosphoproteomics: The raw proteomic mass spectrometry data files were processed using Proteome Discoverer software v1.4 (Thermo Scientific) and searched against the UniProt Human database (134,169 entries) using the SEQUEST algorithm. Peptide precursor mass tolerance was set at 10ppm, and MS/MS tolerance was set at 0.6Da. Search criteria included carbamidomethylation of cysteine (+57.0214) as a fixed modification and oxidation of methionine (+15.9949) and phosphorylation of serine, threonine and tyrosine (+79.966Da) as variable modifications. Searches were performed with full tryptic digestion and a maximum of 1 missed cleavage was allowed. The reverse database search option was enabled and all peptide data was filtered to satisfy false discovery rate (FDR) of 1%.

Proteomic Data Analysis

Resulting proteomics data was analysed with Gitools 2.2.2 and the STRING database. For Gene Ontology (GO) term enrichment analysis, a fold change matrix was created from the protein expression datasets and imported into the Gitools framework 2.2.2 for SLEA analyses(1). Modules for gene annotations, GO terms and KEGG pathways were downloaded from the Ensembl database(2). TMT datasets were clustered with the use of Cluster 3.0(3), via average-link hierarchical clustering. The resulting dendrograms and heatmaps were visualized with the use of Java TreeView 1.1.6r4(4). The proteomic data set was submitted into Ingenuity Pathway Analysis (IPA; Qiagen, Hilden, Germany) for core analysis and functional network analysis. The mass spectrometry proteomics data have been deposited to the ProteomeXchange Consortium via the PRIDE(5) partner repository with the dataset identifiers PXD009015, PXD009023 and PXD009024.

Fixed-cell Immunofluorescence

For the respective experiments, Mitotracker® Deep Red FM was used as a mitochondrial selective probe (Thermo Fisher Scientific) and phosphatidylserine (PS) was labelled using the Annexin-V-FLUOS Staining Kit (Roche, Basel, Switzerland). Cells were fixed in 1% PFA and 0.0075% V/V Glutaraldehyde in PBSAG for 15 min at RT. All washes were carried out in PBSAG. Once fixed, cells were washed twice and permeabilised in 0.05% Triton (Fluka BioChemika, Buchs, Switzerland) for 5 min at RT. After permeabilization, the cells were incubated for blocking in a PBSAG solution of 4% w/V BSA during 30 min at RT, washed once,

incubated for 1 hour at RT with the desired primary antibodies, washed in triplicate and then incubated with suitably labelled secondary antibodies for 1 hour at RT in the dark. The cells were washed in triplicate and an appropriate amount was cytospun onto glass slides, which were then mounted using Mowiol. Confocal images were taken using a Leica SP5 confocal microscope with 63x/1.4 NA oil-immersion lens (Wolfson Bioimaging Facility, Bristol, UK) and processed using Fiji/ImageJ(6).

Trypsin Treatment for Internalized Glycophorin A Detection

Filtered reticulocytes were washed 3 times prior to resuspension in a 1:4 ratio of packed cells to trypsin (2.5mg/ml) PBS solution and incubated with rotation at 37ºC for 30 min. Cells were removed from the trypsin PBS by 4 washes with PBSAG. After treatment, the fixed-cell immunofluorescence protocol was followed using an anti-GPA (clone R10) antibody.

Live-cell Immunofluorescence

Cells were incubated in a PBS solution containing 5% FBS (GE Healthcare), 5µM Calcein Blue AM (Thermo Fisher Scientific) and 500nM Mitotracker® Deep Red FM (Thermo Fisher Scientific) for 30 min at 37ºC, 5% CO_2. After incubation, the cells were washed twice with PBS + 5% FBS and resuspended in tertiary culture medium. 100µl of cell suspension (corresponding to 10^5 cells) were set in a glass bottom culture dish and imaged at 37ºC, 5% CO_2 using a Leica SP8 confocal microscope with 63x/1.4 NA oil-immersion lens (Wolfson Bioimaging Facility). Images were processed using Vision4D (arivis, Rostock, Germany).

Automated Image Processing

Tile scans composed of 10x10 images taken at 1024x1024 resolution were generated via confocal imaging and analysed via arivis Vision4D (arivis). The following steps were used for dataset analysis:
Denoising filter applied to the Calcein Blue channel with mean filter, Radius 3 for background reduction; Background correction applied to the Mitotracker channel with Preserve Bright selected for background reduction, as the background in the far-red channel was typically uneven along the tile scan; Denoising filter applied to the Mitotracker channel with mean filter, Radius 1 for background reduction; Results stored for further analysis.
Cell segments generated from the Calcein Blue channel using an intensity threshold from 8-255 pixel intensity; Mitochondria segments generated from the Mitotracker channel using an intensity threshold from 59-255 pixel intensity; Cell segments filtered based on area

(Projection (XY/Z): Area > 25µm^2), roundness (Projection (XY/Z): Roundness>0.1) and sum of Mitotracker channel intensities (Sum of intensities < 10^6) to remove non-cell segments based on size and autofluorescence in the far-red channel; Mitochondria segments filtered based on area (Area between 0.1µm^2 and 20µm^2) to remove non-related objects;
Segment colocalization applied with cell segments as subjects and mitochondria segments as references, with colocalization measure of partial coverage;
Annotations resulting from the filtering and colocalization steps were stored in tables at the end of processing.

Circulation System Assembly

To create a suitable loop for reticulocyte circulation, a length of 20cm of Pharmed® BPT tubing (Size 13, Inner Diameter 1.6mm; Cole Parmer) was connected to a three-way stopcock (CODAN Steritex ApS) with the use of male and female luer fittings with lock ring and hose barb (Cole Parmer). For injection of the cell suspension into the system, a 1ml syringe without needle (Terumo) was used with the three-way stopcock while the system was open to let air out, until all the tubing was filled with the cell suspension. The system was then closed and fitted into a Watson Marlow 120U/DV pump (Cole Parmer).

Sodium Dodecyl Sulphate Polyacrylamide Gel Electrophoresis (SDS-PAGE)

Cells for lysis were centrifuged at 300g for 5 min. The supernatant was removed and the cells were resuspended at 1x10^6 cells/10µl in cold lysis buffer (supplemented with 1:100 200mM PMSF, 1:100 anti-protease cocktail and 0.0184g Na_3VO_4 per 10ml lysis buffer). Samples were then incubated on ice for 10 min and the lysate was cleared through centrifugation for 10 min at 15871g, 4ºC to remove debris and cell membranes. Proteins were separated using sodium dodecyl sulphate polyacrylamide gel electrophoresis (SDS-PAGE), which was performed with a Mini PROTEAN® Tetra gel electrophoresis system (BioRad, Hercules, USA). Resolving gels were prepared with the use of 6% (w/V) acrylamide (Severn Biotech, Kidderminster, UK), 0.4M Tris-HCl (pH 8.8) and 0.1% SDS. Acrylamide polymerisation was initiated by addition of 0.4% N,N,N,N–Tetramethylene-diamine (TEMED) and 0.1% ammonium persulphate (APS). The stacking gel, placed above the resolving gel, was prepared with 5% (w/V) acrylamide, 0.13M Tris-HCl (pH 6.8), 0.1% SDS, 0.1% APS, and 0.1% TEMED.

Sample buffer (50mM Tris-base pH 8, 12% (w/V) glycerol, 10% SDS, 2mM EDTA, 10% dithiothreitol [DTT]) was used to load the lysates into the gel after incubation at 95°C for 30

seconds. A prestained protein standard, Spectra Multicolor High Range Protein Ladder (Thermo Fisher Scientific, Waltham, USA), was run alongside the samples for molecular weight calibration. Electrophoresis was performed at 25mA in SDS-PAGE Running Buffer (190mM glycine, 25mM Tris-base, 0.1% (w/V) SDS) until the dye front reached the bottom of the gel.

Western Blotting

Resolved proteins were transferred from the polyacrylamide gel to a polyvinylidene fluoride (PVDF) membrane (Millipore). The PVDF membrane was pre-incubated in methanol for activation and equilibrated in transfer buffer (39mM Glycine, 48mM Tris-base, 1.3mM SDS in 20% V/V methanol). The membrane was then layered above 4 sheets of 3MM Whatman paper, also pre-incubated in transfer buffer. The gel was then placed on the PVDF membrane and covered with 4 more sheets of pre-soaked 3MM paper. The proteins were then transferred using a Semi-Dry Blotting transfer unit TE77 PWR (GE Healthcare, Chicago, USA) set at 45mA per gel for a minimum of 1 hour.

SUPPLEMENTAL REFERENCES

1. Perez-Llamas C, Lopez-Bigas N. Gitools: analysis and visualisation of genomic data using interactive heat-maps. PLoS One. 2011;6(5):e19541.
2. Zerbino DR, Achuthan P, Akanni W, Amode MR, Barrell D, Bhai J, et al. Ensembl 2018. Nucleic Acids Res. 2018 Jan 4;46(D1):D754-D61.
3. de Hoon MJ, Imoto S, Nolan J, Miyano S. Open source clustering software. Bioinformatics. 2004 Jun 12;20(9):1453-4.
4. Saldanha AJ. Java Treeview--extensible visualization of microarray data. Bioinformatics. 2004 Nov 22;20(17):3246-8.
5. Vizcaino JA, Csordas A, Del-Toro N, Dianes JA, Griss J, Lavidas I, et al. 2016 update of the PRIDE database and its related tools. Nucleic Acids Res. 2016 Dec 15;44(22):11033.
6. Schindelin J, Arganda-Carreras I, Frise E, Kaynig V, Longair M, Pietzsch T, et al. Fiji: an open-source platform for biological-image analysis. Nat Methods. 2012 Jun 28;9(7):676-82.